Analysis of RNA–protein interactions of mouse liver cytochrome P4502A5 mRNA

Anne TILLOY-ELLUL*[1], Francoise RAFFALLI-MATHIEU†[1], and Matti A. LANG†[2]

*International Agency for Research on Cancer, 150 Cours Albert Thomas, 69372, Lyon Cedex 08, France, and †Department of Biochemistry, Faculty of Pharmacy, Biomedical Centrum, Box 578, University of Uppsala, Uppsala, Sweden

In our previous studies we have identified a 37/39 kDa, pyrazole-inducible, cytochrome P4502A5 (CYP2A5) mRNA binding protein and provided evidence that it may play a role in the stabilization and processing of the RNA [Geneste, Rafalli and Lang (1996) Biochem. J. **313**, 1029–1037; Thulke-Gross, Hergenhahn, Tilloy-Ellul, Lang and Bartsch (1998) Biochem. J. **331**, 473–481]. Details of the RNA–protein interactions are, however, not known. In this report we have performed an analysis of the interaction between the CYP2A5 mRNA and the 37/39 kDa protein. With UV-cross linking experiments, using RNA probes corresponding to various parts of the CYP2A5 mRNA, and with antisense oligonucleotides complementary to certain areas of the 3′-untranslated region (3′UTR), we could map the primary binding site to the tip of a 71 nt hair-pin loop at the 3′-UTR. This analysis also showed that the protein may have more than one site of interaction with the RNA and/or that, within the binding region, there could be more than one protein molecule binding to the RNA. Analysis of the probable conformations of the various probes used in the UV cross-linking experiments, in combination with the estimated binding affinities of the protein to the different probes, suggests that important factors in the high-affinity binding are the UAG triplet flanked by GA-rich sequences at the tip of the hair-pin loop, in addition to the conformation of the loop itself. Within the binding region, similarities with known binding sites of heterogeneous nuclear ribonucleoprotein (hnRNP) A1 in other RNA molecules were revealed by sequence alignment analysis. Moreover, competition experiments with an oligoribonucleotide corresponding to a known high-affinity binding site of hnRNP A1, and immunoprecipitation of the UV cross-linked 37/39 kDa complex showed that the protein binding to the CYP2A5 mRNA could be hnRNP A1 or its close analogue. It was also shown that the 37/39 kDa protein binds with less affinity to CYP2A4 mRNA than to CYP2A5 mRNA. This is in accordance with experiments characterizing the binding site, since these two otherwise highly homologous genes are kown to have a three nucleotide difference within the region important for the high binding affinity. Since the response of CYP2A4 to pyrazole is known to be weak, as compared with CYP2A5, this observation provides further evidence for a regulatory role of the 37/39 kDa protein in CYP2A5 mRNA metabolism.

Key words: conformation, consensus sequence, 3′-untranslated region, heterogeneous nuclear ribonucleoprotein A1, UV cross-linking.

INTRODUCTION

Cytochromes P450 (CYPs) are a superfamily of haemoproteins catalysing various oxidation reactions of drugs and other xenobiotics as well as endogenous compounds [1,2]. Biotransformation of xenobiotics is catalysed mainly by CYPs belonging to families 1–3 and it has been well documented that most of them are inducible and can be regulated by different mechanisms [3]. For some of them, regulation of expression appears to be very complex, involving both transcriptional and post-transcriptional events [4,5]. In spite of many reports dealing with the induction of drug metabolizing CYPs, surprisingly little is known about the exact molecular mechanisms of the regulation, particularly at the post-transcriptional level.

In order to investigate the detailed molecular events involved in the regulation of CYPs, and their induction by environmental stress, we have chosen mouse liver CYP2A5 as a model. We have shown that this enzyme is induced by a variety of xenobiotics of unrelated structures, and that, depending on the compound, upregulation may take place either transcriptionally or post-transcriptionally via mRNA stabilization [6–9]. We have also identified proteins binding in a specific manner to certain parts of the CYP2A5 mRNA and shown that induction of *Cyp2a5* by pyrazole (PY), a hepatotoxic drug stabilizing CYP2A5 mRNA, is associated with an increased binding of some of the proteins to the mRNA, and with elongation of its poly (A) tail. On the other hand, induction of CYP2A5 by a transcriptional activator, phenobarbital, neither increases the activity of the CYP2A5 mRNA binding proteins nor the size of the poly (A) tail [10,11]. These results have therefore led us to propose that the RNA binding proteins whose activity is increased by PY, and which can be found both in the nucleus and the cytoplasm of hepatocytes, may play a role in the regulation of the *CYP2A5* gene via stabilization and processing of the corresponding RNA [11].

Recently we have partially characterized the major, PY-inducible protein and located its binding site to a 71 nt region at the 3′-untranslated region (3′-UTR) of CYP2A5 mRNA [10]. The binding appears specific to CYP2A5 mRNA, but no detailed analysis of the binding site nor of factors contributing to the high-affinity binding has been carried out. In view of the potential importance of this protein in the regulation of the expression of CYP2A5, such an analysis would be useful in order to provide a better understanding of the regulatory mechanism and how possible modifications in the structure of the mRNA or the

Abbreviations used: CYP, cytrochrome P450; CYP2A5, cytochrome P4502A5; DTT, dithiothreitol; hnRNP, heterogeneous nuclear ribonucleoprotein; 3′UTR, 3′untranslated region; ODN, antisense oligonucleotide; PY, pyrazole; UV-XL, UV cross-linking.

[1] These two authors contributed equally to this work.

[2] To whom correspondence should be addressed (e-mail Matti.Lang@farmbio.uu.se).

protein may affect their interaction and, consequently, expression of the gene.

In this work we have identified and characterized the primary binding site of the major PY-inducible protein at the 3′-UTR of CYP2A5 mRNA and shown that, in addition to the sequence, a particular conformation of the mRNA is necessary for the high binding affinity. We also show that the sequence of the binding site is similar to that of the heterogeneous nuclear ribonucleoprotein A1 (hnRNP A1) binding sites in some other RNAs and we present evidence that the PY-inducible protein might indeed be hnRNP A1, or its close analogue. Finally we show that the protein has apparently reduced affinity for the CYP2A4 mRNA, which has a three nucleotide difference at the primary binding site and only a weak response to PY as compared with CYP2A5.

EXPERIMENTAL

Male DBA/2N mice, 6–8 weeks old, were provided by Charles River, Sulzfed, Germany. They were given PY (150 mg/kg) in PBS as intraperitoneal injections for three consecutive days and killed after the last injection. The liver was removed and the microsomal fraction was prepared as described previously [11] and suspended in a storage buffer containing protease inhibitors as follows: 250 μg/ml Prefabloc, 5 μg/ml leupeptin, 5 μg/ml pepstatin and 1 μg/ml aprotinin (Boehringer, Mannheim, Germany). Microsomes were stored in small aliquots at −80 °C and the same batch of microsomal proteins was used in all experiments. The crude cytoplasmic fracion was prepared as described previously [10].

Preparation of radiolabelled RNA probes

Using different sets of primers, segments of various parts of CYP2A5 cDNA were produced (see Figure 1) by PCR amplification as previously described [11,12]. Sense oligonucleotides contained, at the 5′end, 23 nucleotides corresponding to the T7 RNA polymerase promoter. PCR-amplified products were transcribed with T7 RNA polymerase in the presence of [α-^{32}P]UTP or [α-^{32}P]ATP (800Ci/mmol; ICN), following the manufacturers's instructions (Promega, Madison, WI, U. S.A). Transcripts were separated from unincorporated nucleotides by microdialysis on Millipore filters, type VS (0.2 μm pore size). The specific activities of the different probes were calculated by trichloroacetic acid precipitation (following the instructions of Promega) and were in the range of 1.8×10^8–2.5×10^8 c.p.m./μg of transcript. The quality of the RNA probes was checked on a 5% polyacrylamide gel containing 2.3 M urea using standard conditions. The probes with the various 5 nt deletions were produced with appropriate primers covering the site of deletion. To verify the structure, sequencing of the products was performed before *in vitro* transcription.

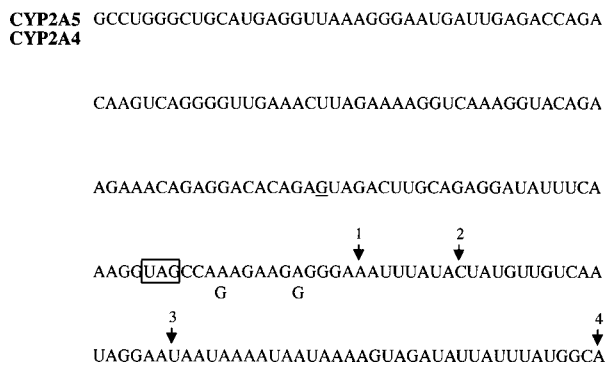

Figure 1 Sequence of the entire 3′-UTR of CYP2A5 mRNA (205 nt) and CYP2A4 mRNA

The probes, corresponding to parts of the CYP2A5 3′-UTR, used in the UV cross-linking analyses are indicated: they start at the underlined 'G' and finish at: 1 for the 45 nt, 2 for the 53 nt, 3 for the 71 nt and at 4 for the 105 nt probes. Only those nucleotides that are different in the CYP2A4 sequence are indicated. The UAG motif is shown in a box. For further details see the Materials and methods section.

UV cross-linking assay

Binding reactions were performed as described previously by Geneste et al. [10]. In brief, the reaction was carried out in a volume of 20 μl containing 2–5 μg of microsomal protein, 10^6 c.p.m. of ^{32}P-labelled probe, 10 mM Hepes (pH 7.6), 3 mM $MgCl_2$, 40 mM KCl, 5% (v/v) glycerol, 1 mM dithiothreitol and yeast tRNA (100 ng/μl). After 10 min of incubation at room temperature, the reaction mixture was placed on ice and exposed to UV light for 8 min at a distance of about 10 cm in a Stratalinker apparatus (Stratagene, La Jolla, CA, U.S.A.; UV-lamp BLE-8T312, Spectronics, Westbury, NY, U.S.A.). Subsequently, unbound RNA was digested for 20 min by RNase A (2 μg/μl; Sigma) at 37 °C. Proteins were separated by SDS/PAGE (12% gel) under non-reducing conditions. Gels were dried and exposed to Fuji RX films with intensifying screens at −80 °C. Quantification of the band intensities was performed by densitometric analysis with a GS 670 Imaging Densitometer (Bio-Rad, Hercules, CA, U.S.A.).

In experiments with antisense oligonucleotides (ODNs; Genset, Paris, France), various amounts of oligonucleotides (as indicated in Figure 4) were pre-mixed with the ^{32}P-labelled RNA probe to allow base pairing for 5 min before the addition of the microsomal protein.

For competition experiments, 10^6 c.p.m. of probe (corresponding to approx. 4.0 ng of radiolabelled transcript) was premixed with increasing amounts of cold competitor before addition of the protein. Subsequent steps were as described above for the UV cross-linking assays.

Immunoprecipitation

The UV cross-linked complex was immunoprecipitated essentially as described by Hamilton et al. [12]. A typical UV cross-linking assay was performed using 2×10^6 c.p.m. of radiolabelled 71 nt probe and 60 μg of cytoplasmic proteins from PY-treated mouse livers. After RNase A digestion, the RNA–protein complexes were incubated with 1:500 dilutions of anti-hnRNP A1 (9H10) or anti-hnRNP C (4f4) monoclonal antibodies for 2 h at 4 °C (antibodies were kindly provided by Dr. G. Dreyfuss, Howard Hughes Medical Institute, University of Philadelphia, U.S.A.).

Precipitation was performed using Protein A–Sepharose beads (Promega). After washing, the proteins were denaturated and analysed by SDS/PAGE (12% gel). Dried gels were autoradiographed for 72 h.

RESULTS

Characterization of the region of CYP2A5 mRNA necessary for the high-affinity binding of the PY-inducible protein

Our previous studies have shown that the primary binding site of the major, PY-inducible protein is located in a 71 nt sequence at the 3′-UTR of the CYP2A5 mRNA [10]. Based on this, we first wanted to investigate what parts of the mRNA are of importance for the complete and high-affinity binding of the protein. For

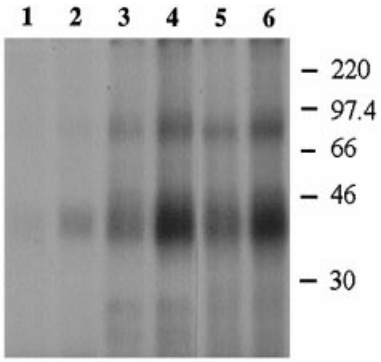

Figure 2 UV cross-linking analysis of the binding of the PY-inducible protein to the 3′-UTR of CYP2A5 mRNA

Analysis was performed with three different probes: the 45 nt (lanes 1 and 2); the 71 nt (lanes 3 and 4) and the full-length (lanes 5 and 6) 3′-UTR using 2 μg (lanes 1, 3 and 5) or 4 μg (lanes 2, 4 and 6) of microsomal protein from PY-treated mouse livers in the incubation mixture. The positions of molecular mass markers are indicated on the right (kDa).

that purpose three probes were used in UV cross-linking experiments: the full-length 3′-UTR, a 71 nt probe and a 45 nt probe containing only part of the 71 nt sequence (see Figure 1). As can be seen in Figure 2, the 71 nt probe shows binding characteristics that are identical with the entire 3′-UTR, but with the 45 nt probe binding activity is dramatically reduced. This result was obtained in repeated experiments with somewhat different protein concentrations and incubation times (results not shown). In some experiments a 105 nt probe (see Figure 1) instead of the 71 nt probe was used, but no difference was found in their binding characteristics (results not shown). These results suggest that the 71 nt sequence not only contains the primary binding site but also displays binding characteristics that are identical with the entire 3′-UTR and could therefore be used in more detailed analysis of the interaction between the major PY-inducible protein and the CYP2A5 mRNA.

Identification and characterization of the primary binding site

Studies with ODNs *in vitro*

To examine the RNA–protein interactions in detail, we first carried out a conformation analysis on the 71 nt probe, which revealed a characteristic hair-pin loop structure as shown in Figure 3. With the help of this analysis three ODNs (I, II, III) were designed, corresponding to different segments of the 71 nt probe, as indicated in Figure 3. These oligonucleotides were used in UV cross-linking competition assays showing that ODN II was by far the most effective one in preventing the protein binding to the RNA (Figure 4). Also, ODN I was able to prevent the complex formation in a dose-dependent manner, although less efficiently than ODN II. In contrast, ODN III had only weak effects on the complex formation, and curiously, with increasing concentrations of ODN III, protein binding seemed to increase as compared with controls without oligonucleotides in the incubation mixture. Also, a scrambled oligonucleotide, with no sequence similarity to the 3′-UTR of CYP2A5 mRNA, increased the binding of the protein to the 71 nt RNA (Figure 4).

UV cross-linking analysis with deleted probes

Analysis with the oligonucleotides suggests that the primary binding site is covered by ODN II, but that some RNA–protein interaction may also take place in the region covered by ODN I. We therefore produced five probes with different deletions (D1–D5) encompassing respectively different parts of the sequence complementary to ODN II and two nucleotides upstream of the ODN I covered sequence, as shown in Figure 5. UV cross-linking analysis showed that deletions D1 and D2 did not change the binding activity much, compared with the non-deleted probe. In contrast, the D4 probe displayed only weak binding, and with the D5 probe the binding activity was strongly reduced (Figure 6). Surprisingly, the D3 probe displayed an increased binding activity compared with the non-deleted probe (Figure 6).

These results are in agreement with those obtained with ODNs and suggest that the primary binding site of the major PY-inducible protein at the 3′-UTR of CYP2A5 mRNA lies within the 5 nt deleted segment of the D4 probe, but that flanking regions may also play a role in the protein–RNA interactions (see Figures 3 and 5).

Examination of the sequence covered by deletions D1–D5 shows that it contains only two UMP nucleotides: one in D4 and one in D5 (see Figure 5). On the other hand AMPs can be found within all deletions (see Figure 5). Since [α-^{32}P]UTP was used in most experiments to prepare the radiolabelled probes, we also wanted to prepare probes labelled with [α-^{32}P]ATP, in order to see whether this might affect the apparent binding pattern shown with the UV cross-linking analysis. It appeared that the binding patterns with the [^{32}P]ATP- and [^{32}P]UTP-labelled probes were similar but not identical (Figure 7). An apparently stronger binding was obtained when probes were labelled with [α-^{32}P]ATP than with [α-^{32}P]UTP. This may not be surprising considering the larger number of radiolabelled nucleotides incorporated in the putative binding region. In any case, the D4 probe displayed the weakest binding activity, further suggesting that the primary binding site is located within the deleted 5 nt. Also, the increased binding activity displayed by the D3 probe compared with the wild type, could be demonstrated with both labels. This suggests that the D3 deletion has created an artificial binding site for the protein, with enhanced affinity.

Depending on the gel and the running conditions, it appears that the UV cross-linked complexes can be separated into two bands of approx. 37/39 kDa (see Materials and methods section and [11]). This is clearly shown, e.g. in Figure 4. The 37/39 kDa bands are also shown in Figure 7. Interestingly, a duplicate band of equal intensity appears only with the non-deleted (wild-type) and the D3 deleted probes. With the D2 probe the predominant band obtained is 37 kDa, whereas with the D4 probe the predominant band is 39 kDa (Figure 7).

Although preliminary, these results could suggest that the protein has multiple sites of interaction with the RNA: one in the D4 region and another one in the D2 region. Alternatively, two protein molecules could be binding to the RNA at different sites. In any case these results demonstrate the importance of the tip of the hair-pin loop for protein binding (see e.g. Figure 5).

Evidence that the PY-inducible protein binding to CYP2A5 mRNA is related to hnRNP A1

Sequence analysis of the 37/39 kDa protein binding region

To characterize further the RNA–protein interaction, a sequence alignment comparison of the binding region of the 37/39 kDa protein was carried out. Interestingly this analysis showed that the tip of the hair-pin covered by ODN II, including the primary binding site, contains a UAG triplet and an AG-rich sequence, which are also found in some known binding sites of the hnRNP A1 [13–15]. Furthermore, the D3 deletion leading to enhanced cross-linking of the 37/39 kDa protein creates a UAGGA motif

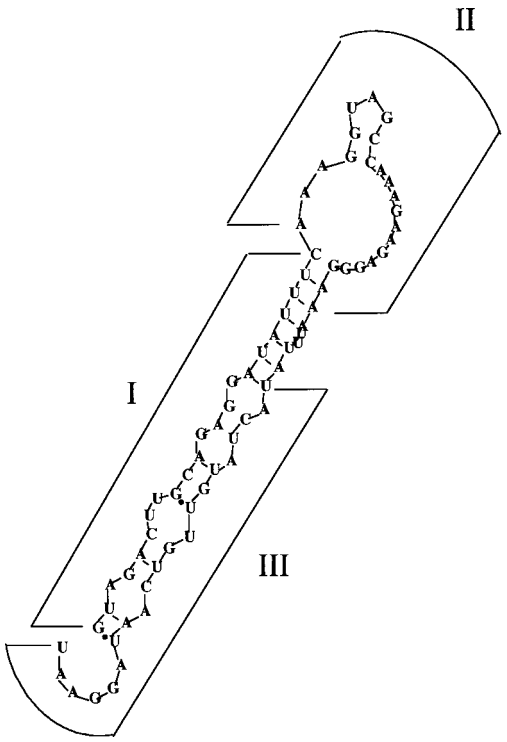

Figure 3 Predicted secondary structure of the 71 nt probe (RNA draw software) and positions along the probe of the three ODNs I, II and III used in the UV cross-linking analysis

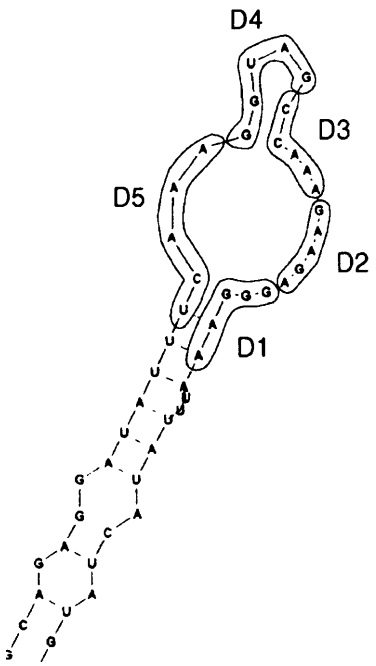

Figure 5 Predicted secondary structure of the tip of the 71 nt probe

The sites of deletions D1–D5 are indicated.

with increased sequence similarity to the hnRNP A1 high-affinity binding site (UAGGGA/U), as defined by Burd and Dreyfuss [13].

Competition with a hnRNP A1-binding sequence

Next, we performed competition experiments with a synthetic oligoribonucleotide containing a sequence to which hnRNP A1 binds with a very high affinity, but which has not been found in any natural RNA. This sequence is called the 'winner sequence'

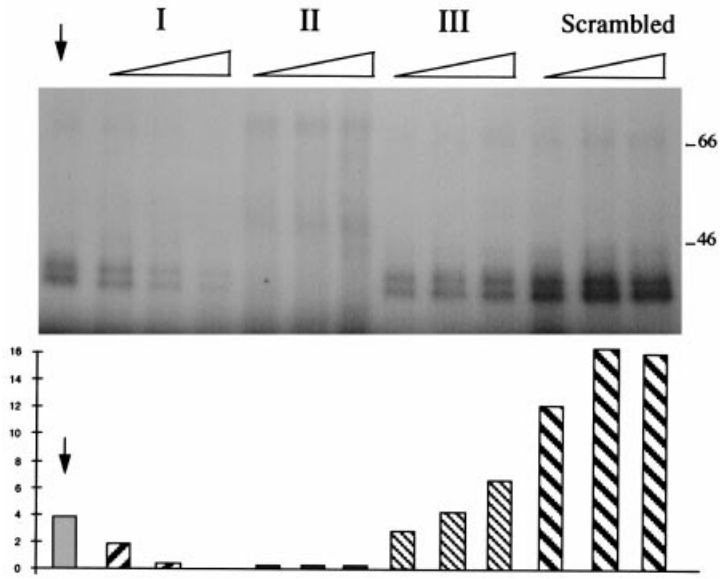

Figure 4 Effect of ODNs I, II and III and a scrambled oligonucleotide on the protein binding to the 71 nt probe as analysed by UV cross-linking

Increasing amounts of each oligonucleotide: 3-, 6- and 12-fold molar excess relative to the radiolabelled probe, were added to the incubation mixture 5 min before adding 4 μg of the microsomal protein preparation from PY-treated mouse livers. The lane indicated by an arrow shows the level of binding without oligonucleotide in the incubation mixture (control). Densitometric analysis of the relative intensity of the 37/39 kDa band is shown below. The positions of molecular-mass markers are indicated on the right. The y-axis units are relative band intensity.

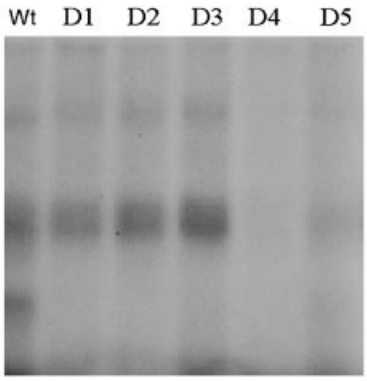

Figure 6 UV cross-linking analysis of protein binding to the non-deleted wild-type (Wt) probe and to probes with deletions D1–D5

Each probe (10^6 c.p.m.) was incubated with 3 μg of microsomal protein from livers of PY-treated mice. For further details see Materials and methods section.

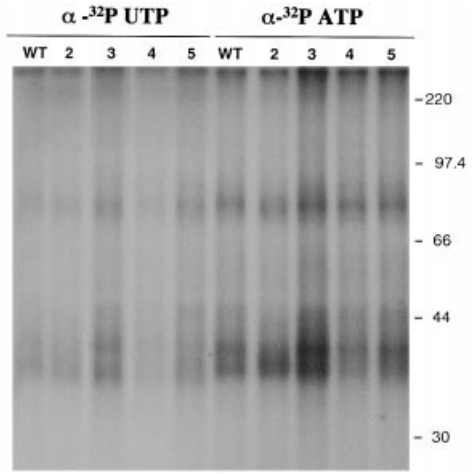

Figure 7 UV cross-linking analysis of microsomal protein binding to the 105 nt probe (WT) and to D2–D5 deleted 100 nt probes labelled either with [^{32}P]UTP or with [^{32}P]ATP

Microsomal protein (3 μg) was incubated with probes corresponding to 10^6 c.p.m. The positions of molecular-mass markers are indicated on the right (kDa).

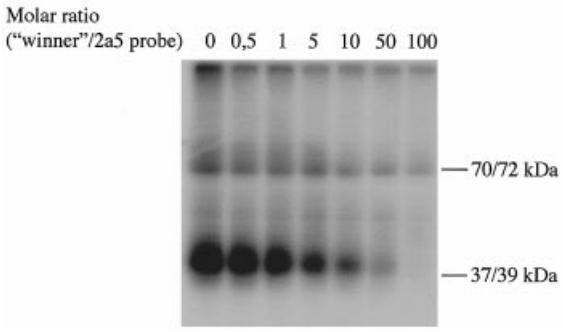

Figure 8 Competition with the 'winner' oligoribonucleotide

UV cross-linking reactions were performed in the presence of increasing amounts of the 'winner' oligoribonucleotides. Molar ratios ('winner'/CYP2A5 probe) of 0, 0.5, 1, 5, 10, 50 and 100 were used. The positions of molecular-mass markers are indicated on the right.

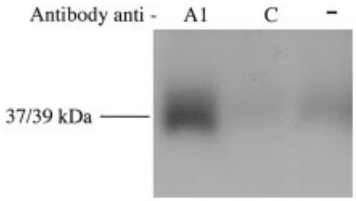

Figure 9 Immunoprecipitation of the 37/39 kDa complex

The RNA–protein complexes from UV cross-linking mixtures were immunoprecipitated with anti-hnRNP A1 antibody 9H10 and the anti-hnRNP C antibody 4F4. A control reaction with no antibody was carried out for comparison.

by Burd and Dreyfuss [13]. Crude cytoplasmic proteins from mouse liver were UV cross-linked to the radioactive 71 nt probe (see Figure 1) in the presence of increasing amounts of the 'winner' 20-mer RNA and a specific and dose-dependent inhibition of the formation of the 37/39 kDa complex was observed (Figure 8). In contrast, the intensity of the 70/72 kDa complex remained largely unaffected by the competitor.

Immunoprecipitation of the 37/39 kDa protein–RNA complex

The protein in the 37/39 kDa complex was identified by a monoclonal antibody directed against hnRNP A1. After performing a typical UV cross-linking reaction with proteins from mouse liver crude extract, an immunoprecipitation with antibodies recognizing hnRNP A1 (9H10) or hnRNP C (4F4) (Figure 9) was carried out. We observed that a 37/39 kDa RNA–protein complex was specifically immunoprecipitated by the anti-hnRNP A1 antibody, indicating that the 37/39 kDa protein could be hnRNP A1 or a closely related protein.

Conformation analysis of probes used to study RNA–protein interaction

Several putative high-affinity binding sites of the hnRNP A1 contain UAG and/or AG(G) triplets or motifs resembling the UAGGGA/U sequence. Nevertheless there seem to be only a rather poor overall sequence homology among the targets of hnRNP A1 in the various RNA molecules analysed [14]. Moreover, the highest affinity, 'winner' sequence, which contains a duplication of the UAGGGA/U motif separated by two nucleotides, has so far not been found in any naturally occuring RNAs. On the other hand, it has been proposed that the extremely high affinity of hnRNP A1 for this sequence could be due to its particular conformation in solution [16]. We therefore wanted to know if parameters, other than the sequence, particularly conformation of the RNA, could explain the apparently different affinity of the PY-inducible 37/39 kDa protein for the various probes. For that purpose we performed conformation analysis of all probes used in the UV cross-linking experiments. Figure 10 shows that a hair-pin loop structure with the UAG triplet at the tip of the pin is characteristic for the 71 nt and 105 nt probes, displaying high-affinity binding. Similar structure (although with a shorter stem) is also maintained in the corresponding region of the full-length 3′-UTR. On the other hand, the 45 nt probe with reduced binding affinity seems to form a modified hair-pin loop where the UAG triplet is not located at the tip of the pin but rather at the stem (Figure 10). These results seem to indicate that for the high-affinity binding, a certain hair-pin loop structure with the UAG at the tip of the pin is important.

In addition, probable conformations of the deleted 100 nt

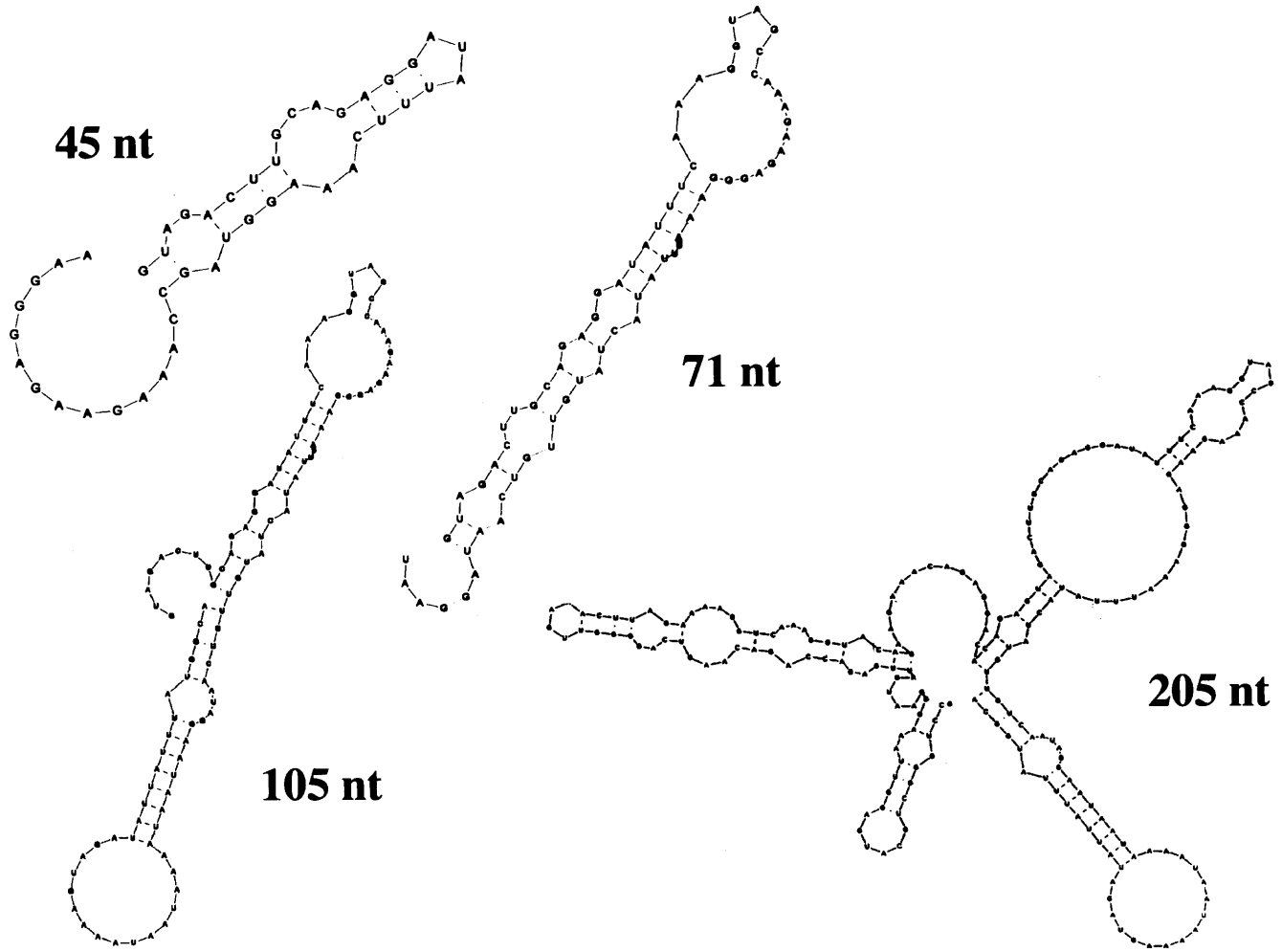

Figure 10 Predicted secondary structures of the 45 nt, 71 nt, 105 nt and the 205 nt (full-length 3′-UTR) probes used in the UV cross-linking analysis

D1–D5 probes are shown in Figure 11, where it appears that the probes with highest conformation similarities are the wild type, D1 and D2. The D3 probe shows a modified hair-pin loop, and after D4 and D5 deletions the probable conformations show major differences compared with the wild type. This, together with the binding-affinity results, further suggest that for the high-affinity binding, a characteristic hair-pin loop, including the UAG triplet, is important. The shift in the position of the triplet at the tip of the loop in the case of D3 seems to be compensated for by creating an artificial high-affinity binding site (see Figure 11). Furthermore, it seems that the AG-rich sequences flanking the UAG triplet contribute to the binding.

Binding of the PY-inducible protein to CYP2A4 and CYP2A5 mRNA

Mouse liver CYP2A4 has extremely high homology with CYP2A5, but only a weak response to PY. Based on Figure 1, it appears that CYP2A4 has two point mutations and one nucleotide deletion, compared with CYP2A5, at or near the important binding region, as described above. Therefore, UV cross-linking analysis was performed using CYP2A4 3′-UTR instead of CYP2A5 3′-UTR as a probe. Based on the UV cross-linking competition assay, as shown in Figure 12, it appears that the PY-inducible protein has a somewhat higher affinity for the CYP2A5 probe than for the CYP2A4 probe, which suggests that the three nucleotide differences could be relevant to the binding affinity.

DISCUSSION

In our investigations on the mechanism of regulation of CYP2A5 we have earlier identified an inducible 37/39 kDa protein binding to the 3′-UTR of the corresponding mRNA and given evidence for its role in the stabilization of the mRNA. Interaction of the protein with the RNA and the characteristics of the protein itself are not well known and therefore, in order to understand more fully the molecular mechanisms involved in the regulation of CYP2A5, we performed a detailed analysis of the RNA–protein interaction. We also show that the 37/39 kDa protein could be hnRNP A1 or a closely related polypeptide as: (i) the binding site has properties similar to known binding sites of hnRNP A1 in certain other mRNA molecules; (ii) an oligoribonucleotide corresponding to a high-affinity binding site for hnRNP A1 is able to compete out the Cyp2a5 mRNA from the 37/39 kDa complex; and (iii) the 37/39 kDa protein is immunologically related to hnRNP A1. Furthermore, we show that although there is only a three nucleotide difference in the binding region, the interaction of the 37/39 kDa protein with the 3′-UTR of the PY-

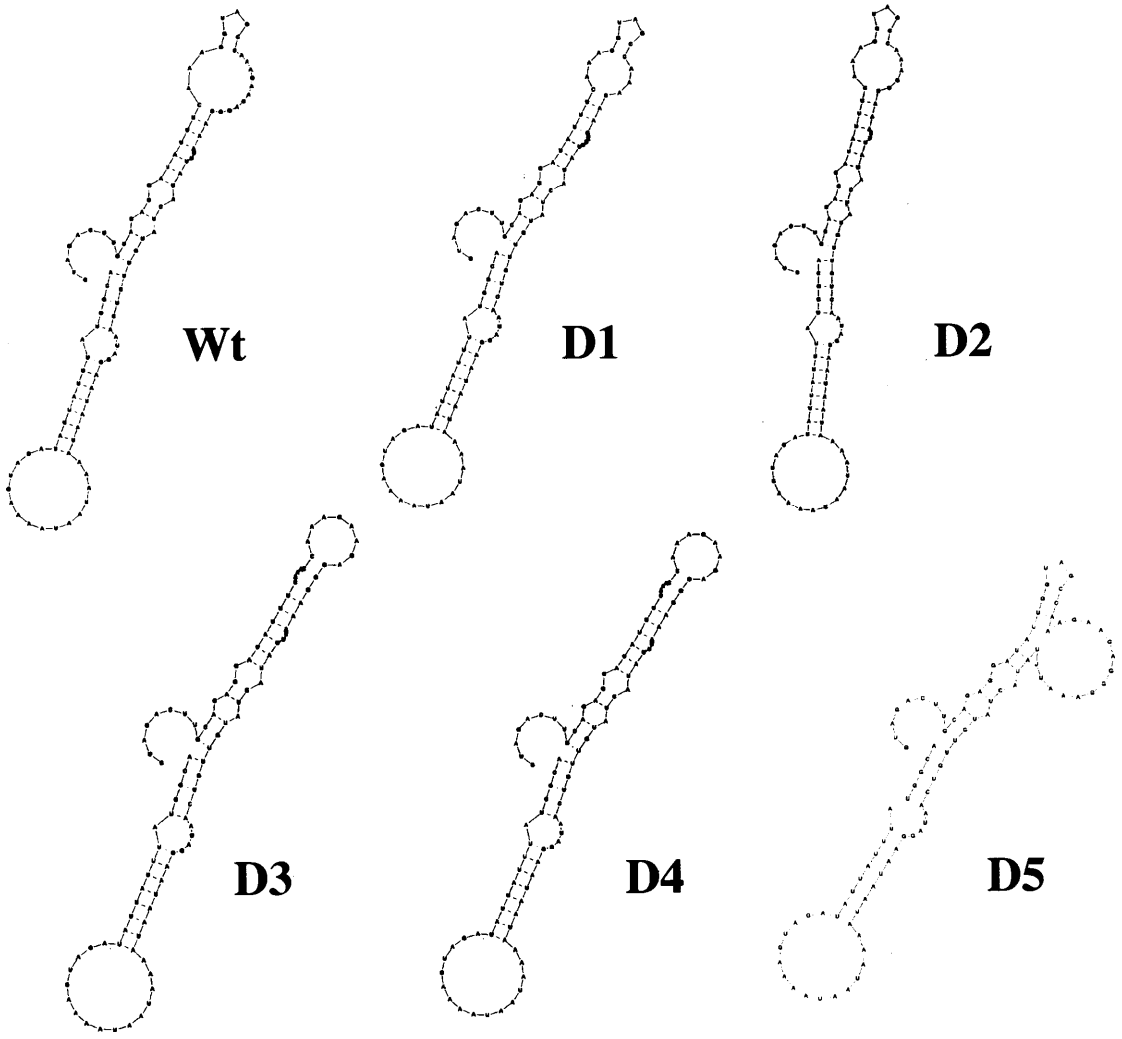

Figure 11 Predicted secondary structures of the wild-type 105 nt (Wt) and 100 nt probes with the respective D1–D5 deletions. (RNA draw software).

inducible CYP2A5 is stronger than with the 3′-UTR of the less responsive CYP2A4, thus providing further evidence of the potentially important role of this protein in the regulation of CYP2A5 expression.

The primary binding site of the 37/39 kDa protein was located at the tip of a putative 71 nt hair-pin loop. Deletion experiments show that the site important for binding contains a UAG triplet flanked by AG-rich regions which are also present in sites corresponding to putative, high-affinity targets of hnRNP A1 [13,14]. Furthermore, the D3 deletion, which increases the binding activity as compared to the native 3′-UTR, has created a motif in the binding region with increased homology to the consensus, high-affinity, binding site of hnRNP A1 (UAGGGA/U) [13]. Taken together, these observations show that the binding site of the 37/39 kDa protein at the 3′-UTR of the CYP2A5 mRNA contains elements that are typical of hnRNP A1 binding sites in other mRNAs, but that it is not identical with any of the hnRNP A1 binding sites described previously. On the other hand, previous studies have shown only relatively little overall sequence homology between hnRNP A1 binding sites in different RNAs [14]. This could mean that whereas certain motifs are important for the binding, other parameters, such as the conformation of the RNA, may contribute to the binding affinity. In this respect, it is important to notice that the probes displaying the highest binding activity, including the native 3′-UTR, have a characteristic hair-pin loop structure.

Several publications have shown that hnRNP A1 is able to both facilitate and destabilize RNA–RNA base pairing [17–19]. This suggests that it is able to affect profoundly the conformation of an RNA. It would therefore make sense for the primary, high-affinity, binding site to be easily accessible, e.g. at the tip of a loop, for the first RNA–protein contact to occur. Subsequent conformational changes could then lead to the final complex formation. Clearly, more work is needed for the complete understanding of the interaction between the hnRNP A1 and the CYP2A5 mRNA.

The duplicate band at 37/39 kDa indicates that two protein molecules are binding to the RNA. However, depending on the probe used, one or two complexes could be detected, suggesting that either two molecules of the same protein with two sites of interaction with the RNA, or two different proteins, interact with the CYP2A5 mRNA. In addition, weaker bands of higher molecular mass were found. This is in agreement with our previous study where a larger, 70/72 kDa, duplicate band, also induced by PY, was discovered [11]. It was shown, however, that whereas the 70/72 kDa protein binds with equal affinity to both

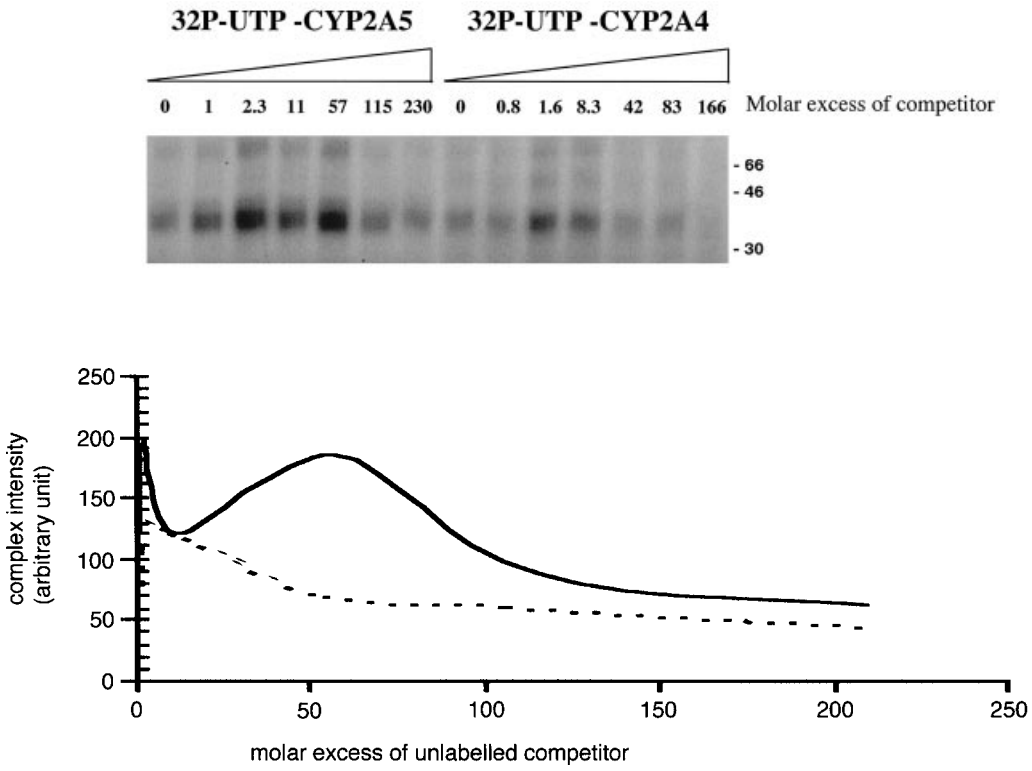

Figure 12 Cross-competition analysis of the binding affinity of the PY-inducible protein to the 3′-UTRs of CYP2A4 and CYP2A5

Top: UV cross-linking. Microsomal protein (5 μg) from PY-treated mouse livers was incubated with [^{32}P]UTP-labelled 71 nt CYP2A5 probe (10^6 c.p.m./0.17 pmol) in the presence of increasing amounts of non-radioactive CYP2A4 3′-UTR RNA, as indicated. In a second series of experiments, the same conditions were used, except that the CYP2A4 RNA was used as a radiolabelled probe and the CYP2A5 RNA as a non-labelled competitor. Bottom: densitometric analysis of band intensities from the top panel. *y*-Axis, relative band intesities where the control level, without competitor, is indicated by 100 arbitrary units; *x*-axis, fold excess of unlabelled competitor. The solid line shows the result for radiolabelled CYP2A5 probe and the dotted line that for the radiolabelled CYP2A4 probe.

c-jun and CYP2A5 mRNA, the 37/39 kDa does not bind to c-jun mRNA. It is possible therefore that despite similar regulation of their binding activity, interaction of the 37/39 kDa and the 70/72 kDa proteins with the RNA is not the same.

Several studies have shown that hnRNP A1 binds not only to nucleic acids, but also to protein molecules. It is found as multimers in hnRNP monoparticles [20]. It binds cooperatively to RNA [21] and has been shown to selectively interact both with itself and with other RNA-binding proteins [22]. In this regard it would be interesting to know whether or not the 37/39 kDa protein interacts with other proteins, including the 70/72 kDa complex, and what relevance this may have for the stabilization and processing of the CYP2A5 mRNA.

Only limited information is available on the interaction of proteins with other CYP mRNAs. We have demonstrated that at least two proteins, one of which presumably is hnRNP C, bind to the 3′-UTR of the CYP1A2 mRNA, and that their binding activity is related to the upregulation of CYP1A2 by 3-methylcholanthrene. The primary binding site of these proteins [a poly (U) region] is different from the primary binding site of the 37/39 kDa protein. In addition, the proteins binding to the mRNA of CYP1A2 seem to be exclusively nuclear [5]. What relation the two CYP1A2 mRNA binding proteins have to the regulation of CYP1A2 expression is currently not known. The 3′-UTR of cholesterol 7-α hydroxylase mRNA has been shown to contain elements regulating the expression of the gene, presumably by affecting the stability or the translational efficiency of the RNA [23]. However, no detailed information on the mechanism, nor of transacting factors interacting with the RNA, is available.

hnRNP A1 is thought to be essential in the regulation of the expression of many genes, and evidence suggest that it can affect gene expression at various stages. For example, it can modulate splicing by promoting distal 5′ splice-site selection [24,25]; in addition it probably plays a role in the nucleocytoplasmic transport of mRNAs [26] and in the regulation of the stablility and translation of mature mRNAs [12,27]. To our knowledge, this is the first report providing evidence for the possible participation of hnRNP A1 in the regulation of a CYP gene. While more work is needed to analyse the protein and factors affecting its activity and regulatory role in detail, this work lays the foundation for our future experiments in trying to understand the mechanism of regulation of CYP genes and how they respond to environmental stress.

We thank Dr. Dreyfuss for providing the monoclonal antibodies against hnRNP A1 and hnRNP C. A. T.-E. was a recipient of a special training award from the International Agency for Research on Cancer.

REFERENCES

1 Nelson, D. R., Kamataki, T., Waxman, D. J., Guengerich, F. P., Estabrook, R. W., Feyereisen, R., Gonzales, F. J., Coon, M. J., Gunsalus, I. C., Gotoh, O. et al. (1993) DNA Cell Biol. **12**, 1–51

2 Lewin, D. F. V. (1996) Cytochromes P450: Structure, Function and Mechanism, pp. 115–167, Taylor & Francis, London
3 Porter, T. D. and Coon, M. J. (1991) J. Biol. Chem. **266**, 13469–13472
4 Wu, D. and Cederbaum, A. I. (1996) Mol. Pharmacol. **49**, 802–807
5 Raffalli-Mathieu, F., Geneste, O. and Lang, M. A. (1997) Eur. J. Biochem. **245**, 17–24
6 Aida, K. and Negishi, M. (1991) Biochemistry, **30**, 8041–8045
7 Hahnemann, B., Salonpää, P., Pasanen, M., Mäenpää, J., Honkakoski, P., Juvonen, R., Lang, M. A., Pelkonen, O. and Raunio, H. (1992) Biochem. J. **286**, 289–294
8 Honkakoski, P., Kojo, A. and Lang, M. A. (1992) Biochem. J. **285**, 979–983
9 Pellinen, P., Stenbäck, F., Rautio, A., Pelkonen, O., Lang, M. A. and Pasanen, M. (1993) Naunyn-Schmiedebergs Arch. Pharmacol. **348**, 435–443
10 Geneste, O., Raffalli, F. and Lang, M. A. (1996) Biochem. J. **313**, 1029–1037
11 Thulke-Gross, M., Hergenhahn, M., Tilloy-Ellul, A., Lang, M. and Bartsch, H. (1998) Biochem. J. **331**, 473–481
12 Hamilton, B. J., Nagy, E., Malter, J. S., Arrick, B. A. and Rigby, W. F. (1993) J. Biol. Chem. **268**, 8881–8887
13 Burd, C. G. and Dreyfuss, G. (1994) EMBO J. **13**, 1197–1204
14 Abdul-Manan, N. and Williams, K. R. (1996) Nucleic Acids Res. **24**, 4063–4070
15 Li, H. P., Zhang, X., Duncan, R., Comai, L. and Lai, M. M. (1997) Proc. Natl. Acad. Sci. U.S.A. **94**, 9544–9549
16 Abdul-Manan, N., O'Malley, S. M. and Williams, K. R. (1996) Biochemistry **35**, 3545–3554
17 Kumar, A. and Wilson, S. H. (1990) Biochemistry **29**, 10717–10722
18 Munroe, S. H. and Dong, X. F. (1992) Proc. Natl. Acad. Sci. U.S.A. **89**, 895–899
19 Cobianchi, F., SenGupta, D. N., Zmudzka, B. Z. and Wilson, S. H. (1986) J. Biol. Chem. **261**, 3536–3543
20 Lothstein, L., Arenstorf, H. P., Chung, S. Y., Walker, B. W., Wooley, J. C. and LeStourgeon, W. M. (1985) J. Cell Biol. **100**, 1570–1581
21 Nadler, S. G., Merrill, B. M., Roberts, W. J., Keating, K. M., Lisbin, M. J., Barnett, S. F., Wilson, S. H. and Williams, K. R. (1991) Biochemistry **30**, 2968–2976
22 Cartegni, L., Maconi, M., Morandi, E., Cobianchi, F., Riva, S. and Biamonti, G. (1996) J. Mol. Biol. **259**, 337–348
23 Agellon, L. B. and Cheema, S. K. (1997) Biochem. J. **328**, 393–399
24 Mayeda, A. and Krainer, A. R. (1992) Cell, **68**, 365–375
25 Caceres, J. F., Stamm, S., Helfman, D. M. and Krainer, A. R. (1994) Science, **265**, 1706–1709
26 Visa, N., Alzhanova-Ericsson, A. T., Sun, X., Kiseleva, E., Bjorkroth, B., Wurtz, T. and Daneholt, B. (1996) Cell, **84**, 253–264
27 Svitkin, Y. V., Ovchinnikov, L. P., Dreyfuss, G. and Sonenberg, N. (1996) EMBO J. **15**, 7147–7155

Received 30 September 1998/25 January 1999; accepted 18 February 1999